Journal of Molecular Liquids 269 (2018) 193–202

Contents lists available at ScienceDirect

Journal of Molecular Liquids

journal homepage: www.elsevier.com/locate/molliq

Inhibitive effect of Clopidogrel as a green corrosion inhibitor for mild steel; statistical modeling and quantum Monte Carlo simulation studies

Ehsan Naseri [a], Mahmoud Hajisafari [a], Ali Kosari [b,c], Mahla Talari [b], Saman Hosseinpour [d,*], Ali Davoodi [b,*]

[a] Department of Metallurgy and Materials Engineering, Yazd Branch, Islamic Azad University, Yazd, Iran
[b] Department of Metallurgical and Materials Engineering, Faculty of Engineering, Ferdowsi University of Mashhad, P.O. Box 91775-1111, Iran
[c] Department of Materials Science and Engineering, Delft University of Technology, Mekelweg 2, 2628 CD Delft, the Netherlands
[d] Institute of Particle Technology (LFG), Friedrich–Alexander–Universität Erlangen-Nürnberg (FAU), Cauerstrasse 4, 91058 Erlangen, Germany

ARTICLE INFO

Article history:
Received 7 March 2018
Received in revised form 4 August 2018
Accepted 8 August 2018
Available online 09 August 2018

Keywords:
Clopidogrel
Green corrosion inhibitor
Mild steel
Sulfuric acid
Surface response method
Monte Carlo simulation
Sum frequency generation (SFG) spectroscopy

ABSTRACT

In this work, response surface method (RSM) is employed to design electrochemical experiments for assessment of a green organic molecule, namely Clopidogrel from cardiovascular drugs class, as a corrosion inhibitor for mild steel in sulfuric acid solution. Mathematical models based on multiple regressions are generated to estimate the influence of the affecting factors like acid concentration, solution temperature and inhibitor concentration on the inhibitive performance of Clopidogrel. The corrosion rates are measured experimentally using potentiodynamic polarization technique. The calculated Langmuir adsorption energy reveals that Clopidogrel adsorbs both physically and chemically onto the mild steel surface and the adsorption type is almost independent of the environmental factors. The adsorption mechanism of Clopidogrel is computed through quantum chemical calculations, confirming that this compound can replace water molecules from the surface upon its adsorption to the metal substrate. The simulation results are approved experimentally using an inherently surface sensitive tool, sum frequency generation spectroscopy (SFG).

1. Introduction

In the case of corrosion prevention in acidic media, the word "organic inhibitor" may be the first expression which passes through one's mind. It is believed that the molecular structure of inhibitors plays an important role in the determination of their adsorption mechanism on metal surfaces. The most efficient inhibitors to date are the compounds comprised of heterocyclic and aliphatic compounds containing heteroatoms like P, S, N, and O in their molecular structures [1,2]. However, the use of some effective inhibitors is banned due to international environmental legislation. Thus, there is a tendency towards introducing and examining new environmentally friendly inhibitors [3–5].

Self-assembled monolayers (SAMs) as simple green coatings are proved to be effective against corrosion of pure metals and simple alloys in indoor and outdoor corrosive atmospheres [5–8]. However, such simple molecules, due to their competitive adsorption with water and other corrosive stimulators, are not applied industrially in the presence of the stream of corrosive media. Nevertheless, the simplicity of SAMs allows important information to be obtained regarding their adsorption and corrosion protection mechanism at a molecular level [9,10]. Based on this fundamental knowledge, recently medical substances and drugs, as more complex corrosion inhibitors than SAMs, attract researchers' and industries' attention. Application of drugs as corrosion inhibitors is very promising as they often have a similar molecular structure to that of the conventional corrosion inhibitors [11,12]. So far, several compounds for different classes of drugs like antibiotics, quinolones, tetracyclines and etc. have been introduced as corrosion inhibitors and their inhibitive performances have been studied, electrochemically and theoretically [12–18]. However, there is a broad range of potential compounds that may effectively act as corrosion inhibitors, but not been investigated yet. Based on its molecular structure, Clopidogrel, from the cardiovascular class of drugs, which is used for heart treatment, is considered to also have a great potential to act as an efficient inhibitor [19–21].

This study aims to investigate the adsorption mechanism and corrosion inhibitive effect of Clopidogrel on mild steel in H_2SO_4 solution. In general, several experimental variables may influence the adsorption behavior, adsorption kinetics, and protection properties of Clopidogrel. However, taking all of the possibly affecting parameters into consideration leads to a large matrix of possible experiments. Thus, current study benefits from the advantages of response surface methodology (RSM) to design a limited number of experiments, with an emphasis on the most influential parameters. Based on the RSM design,

* Corresponding authors.
E-mail addresses: saman.hosseinpour@fau.de (S. Hosseinpour), a.davodi@um.ac.ir (A. Davoodi).

https://doi.org/10.1016/j.molliq.2018.08.050
0167-7322/

potentiodynamic polarization tests are performed to experimentally estimate the corrosion rate in different conditions of temperature, acid and the inhibitor concentrations. In addition, quantum-based Monte Carlo simulation which provide a good atomistic insight into inhibitors/metal interactions are performed. The simulation results are verified experimentally using an inherently surface sensitive spectroscopic technique, sum frequency generation spectroscopy (SFG).

2. Experimental

2.1. Electrochemical evaluations

In this study, St37 steel is used as the substrate and its chemical composition is given in Table 1. The Clopidogrel drug is used as the green inhibitor and it was purchased from Sigma-Aldrich. The chemical composition of Clopidogrel is as $C_{16}H_{16}ClNO_2S$, with its molecular structure depicted in Fig. 1. In this figure, the rings are labeled according to [22]. The acidic media were prepared from dilution of sulfuric acid (Merck 96%) with distilled water. The inhibited solutions were prepared by adding various amounts of Clopidogrel directly to the acidic medium, followed by stirring for 30 min, to obtain homogeneous solutions.

Electrochemical measurements were carried out using a conventional three-electrode cell in which a calomel electrode and a platinum wire were employed as the reference and the counter electrodes, respectively while the mild steel was serving as the working electrode. Prior to the electrochemical measurements, the working electrodes were abraded with emery papers up to 1200 grit. The samples were then washed with distilled water and were dried under the flow of dry air.

Potentiodynamic polarization tests were performed using a Gill AC laboratory potentiostat (ACM Instrument). To approach a steady state condition prior to the potentiodynamic measurements, the samples were immersed for 30 min in the acidic solution and the corresponding open circuit potentials (OCP) were recorded simultaneously. Subsequently, the potentiodynamic polarization tests were performed in the range of ±250 mV with respect to the OCP, at a sweep rate of 1 mV/s. A Bain-marie heated bath with ±1 °C accuracy was used to conduct the experiments at different temperatures.

2.2. Design of experiment

To design the experiments, RSM according to central composite face-centered (CCFD) design was used; the details of which can be found in Ref. [23, 24]. In the inhibited solution, three factors including temperature, acid concentration, and inhibitor concentration were considered, and varied from 25 °C to 45 °C, 0.1 M to 1 M and 200 ppm to 800 ppm, respectively. Accordingly, in total 18 experiments are designed to be performed, as listed in Table 2. In the last column of this table, the corrosion current densities which are estimated, using the potentiodynamic polarization test, are presented. According to Table 3, another set of experiments are designed in order to estimate the steel corrosion rate in the uninhibited solution. These measurements are required for the estimation of inhibitor efficiency and thermodynamic-related calculations in different conditions.

The statistical data were analyzed using Design Expert statistical software (Trial version 7.0), based on the multiple regressions using the least square method. The significance of the terms was evaluated by the variance analysis (ANOVA). ANOVA tables are generated to examine the regression coefficient including linear, quadratic, and interaction. The statistical parameters including, the coefficient of determination (R^2), the adjusted coefficient of determination (R^2_{adj}), and the predicted coefficient of determination (R^2_{pre}) were assessed to evaluate the accuracy of the model. Afterward, the relationship between the independent variables and their response was calculated through the constructed surface plots.

Table 1
Chemical composition of the used St37 steel.

Type	C%	Si%	Mn%	S%	P%	Fe%
ST 37	0.12	–	1.3	0.04	0.031	Balance

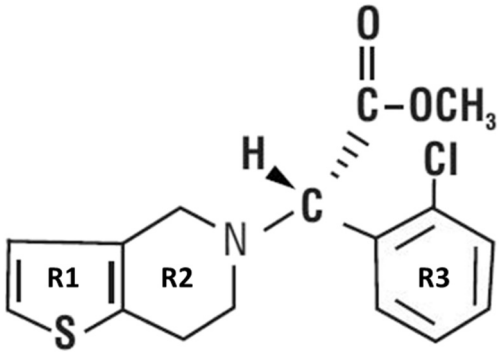

Fig. 1. Chemical structure of the Clopidogrel used as an inhibitor. The ring modes are marked as R1, R2, and R3 according to [22].

2.3. Monte Carlo simulation and verification

In this study, the computational calculations were performed using the Material Studio v 8.0 Accelrys Inc. software. Geometrical optimization of various components was carried out with the generalized gradient approximation (GGA) functional of Becke exchange plus Lee–Yang–Parr correlation (BLYP) in conjunction with double numerical plus d-functions (DND) basis set using $Dmol^3$ module. Fine convergence criteria and global orbital cutoff were used on basis set definitions. To investigate the adsorption behavior of Clopidogrel on Fe (100) plane surface, Monte Carlo (MC) simulations were implemented using the adsorption locator module and COMPASS force field. The simulation was carried out in a simulation box (28.66 Å × 22.93 Å × 56.48 Å) with periodic boundary conditions.

To experimentally verify the results of the MC simulations, SFG measurements were performed at the metal/air interface with deposited Clopidogrel. The theory of SFG spectroscopy and its applications in studying adsorbed molecules as corrosion inhibitors are provided elsewhere [7,25,26]. In brief, when two pulsed laser beams, a tunable IR (ω_{IR}) beam and a visible beam (ω_{Vis}) with a fixed frequency, overlap

Table 2
Range and levels of variables and corresponding response for inhibited solutions.

No.	Type of experiments	Acid concentration (M)	Temperature (°C)	Inhibitor concentration (ppm)	Corrosion current density (mA/cm^2)
1	Factorial points	0.1	25	200	0.13
2		1	25	200	1.01
3		0.1	45	200	0.83
4		1	45	200	3.39
5		0.1	25	800	0.08
6		1	25	800	0.20
7		0.1	45	800	0.39
8		1	45	800	1.84
9	Star points	0.1	35	500	0.08
10		1	35	500	0.74
11		0.55	25	500	0.21
12		0.55	45	500	1.24
13		0.55	35	200	0.77
14		0.55	35	800	0.44
15	Center points	0.55	35	500	0.60
16		0.55	35	500	0.51
17		0.55	35	500	0.67
18		0.55	35	500	0.72

Table 3
Range and levels of variables and corresponding response for uninhibited solutions.

No.	Type of experiments	Acid concentration (M)	Temperature (°C)	Corrosion current density (mA/cm^2)
1	Factorial points	0.1	25	0.52
2		1	25	2.82
3		0.1	45	2.37
4		1	45	12.81
5	Star points	0.1	35	0.87
6		1	35	5.57
7		0.55	25	1.53
8		0.55	45	9.77
9	Center point	0.55	35	2.82
10		0.55	35	3.06
11		0.55	35	3.82
12		0.55	35	3.21

in time and space at an interface, a new electromagnetic wave is generated (ω_{SF}) with its frequency equal to the sum of the frequencies of the incoming beams. The sum frequency (SF) beam includes information from the interfacial molecules, as the inherent symmetry of the molecules in the bulk breaks at interfaces. As for a specific vibration to be SFG active, both Raman and IR activities are required, linear ATR-FTIR and Raman measurements are also performed on pure Clopidogrel. These measurements help with the assignment of the peaks in the SFG spectra. SFG spectrometer used in this study is similar to that used in Ref. [27]. To precisely locate the sample surface and to align it horizontally, a combination of a height sensor (Keyence, LK-G5000) and a He–Ne laser pointer was used. The SFG measurements are performed with all the three beams (i.e. IR, Vis, and SFG) having electric field polarized parallel to the plane of incidence (the PPP polarization combination).

2.4. Corrosion-attack-morphology study

The morphological evolution of a mirror-like steel surface in the course of exposure to inhibited and uninhibited media was studied by optical microscope. Prior to immersion, the sample surface was mechanically polished down to 0.05 μm alumina slurry. The samples were then exposed for 90 min to different sulfuric acid solutions; with and without inhibitor, to evaluate the inhibitor efficiency in different conditions. Afterward, the samples were cleaned ultrasonically in ethanol for 15 min followed by an immediate drying with air flow.

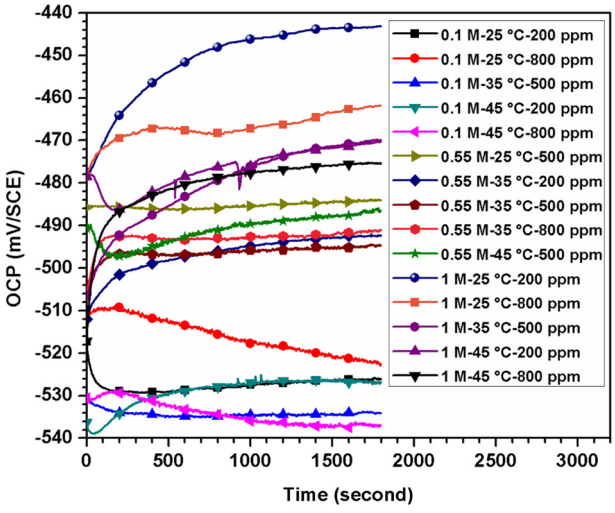

Fig. 2. Corrosion potential variations of the steel in different inhibited solutions as a function of time.

3. Results and discussion

3.1. Inhibited solution

Before each polarization test, the corrosion potential was measured for 30 min to ensure that the system is stabilized. The corrosion potential variations in different conditions, according to Table 2, are shown in

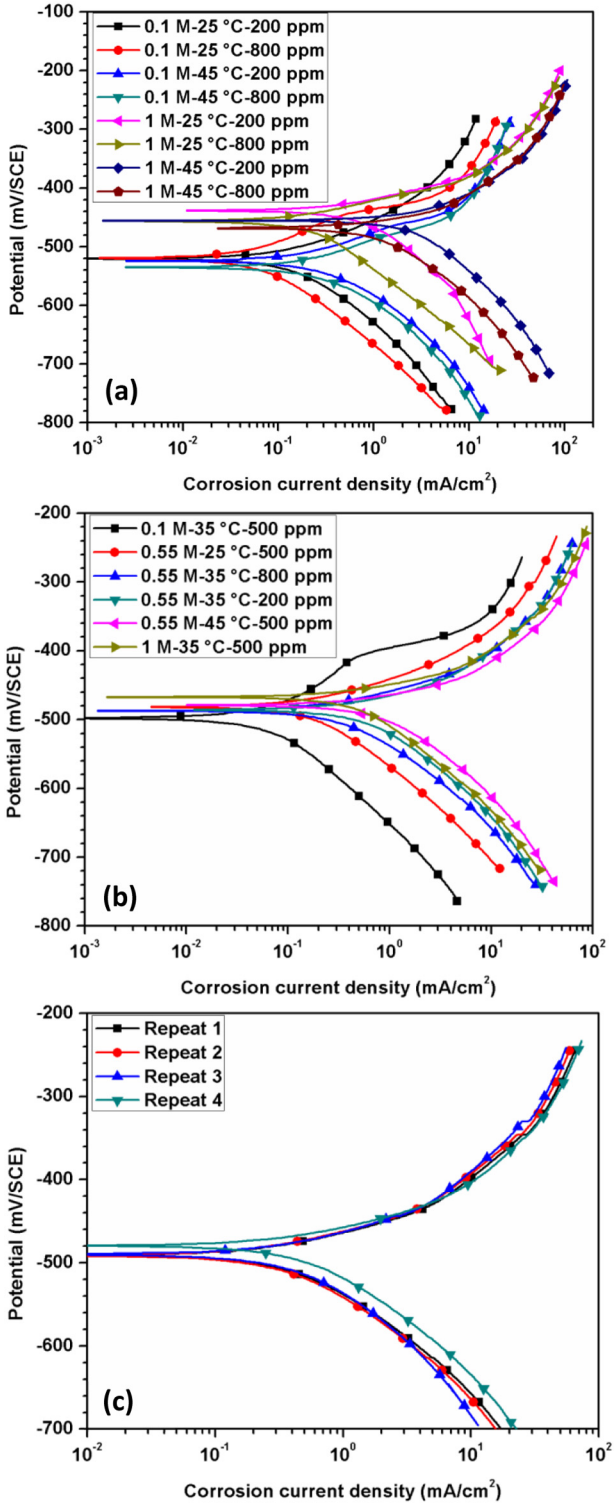

Fig. 3. Polarization curves of the mild steel in the inhibited solutions at the designed (a) factorial points, (b) star points, and (c) center points. The corresponding data can be found in Table 2.

Table 4
Obtained model to calculate the corrosion rate in the inhibited solutions.

Model Corrosion current density (mA/cm^2)	R-squared
$(i_{corr})^{0.5} = -0.18$ $+0.16 \times$ acid concentration $-0.02 \times$ temperature $-2\times10^{-4} \times$ inhibitor concentration $+0.02 \times$ acid concentration $\times$ temperature $-6\times10^{-4} \times$ acid concentration $\times$ inhibitor concentration	0.94

Fig. 2. Based on this figure, in most cases, the system is stabilized after 20 min. We chose the corrosion potential variations less than 10 mV in every 10 min as a criterion for stabilization of the system. As can be seen in Fig. 2, the corrosion potential values are highly dependent on the environmental parameters such as temperature, acid and the inhibitor concentrations, and vary in the range of ~100 mV (−540 to −440 mV).

The potentiodynamic polarization curves of the steel in various conditions of temperature, acid and inhibitor concentrations are presented in Fig. 3. The corrosion rates (i_{corr}), reported in Table 2, are estimated using Tafel extrapolation method. The experimental data are analyzed by the ANOVA method and a mathematical model is introduced in order to calculate the corrosion rate as a function of the experimental conditions. The best parameters which can both mathematically and statistically describe the experimental results are included in the model and are presented in Table 4. The large R-squared values close to one indicate the high level of accuracy of the presented model. To confirm the accuracy of this model, the predicted values from the model are plotted versus the experimental values in Fig. 4.

Fig. 5 illustrates the simultaneous effect of the acid concentration and temperature on the corrosion rate, at 200 and 800 ppm inhibitor concentrations. As is evident from this figure, a simultaneous increase of the acid concentration and temperature dramatically increases the corrosion current density. This effect is more pronounced when the inhibitor is added at the lowest concentration (i.e. 200 ppm). Thus, in a highly aggressive solution, especially at high temperatures, the inhibitor concentration plays a critical role in mitigating the steel corrosion.

Fig. 6 shows the simultaneous effect of acid and inhibitor concentration on the corrosion rate of the st37 steel at 25 °C and 45 °C. According to this figure, at low temperature (top figure), the acid and the inhibitor concentrations do not dramatically influence the corrosion current density. However, at higher temperatures (bottom figure), corrosion rate significantly rises as acid concentration increases. This effect is more noticeable at lower inhibitor concentrations and can be explained by the fact that as the temperature increases, the anodic dissolution in acidic solution is facilitated. Dissolution eventually leads to detachment of the adsorbed inhibitor molecules from the surface (desorption process) [23].

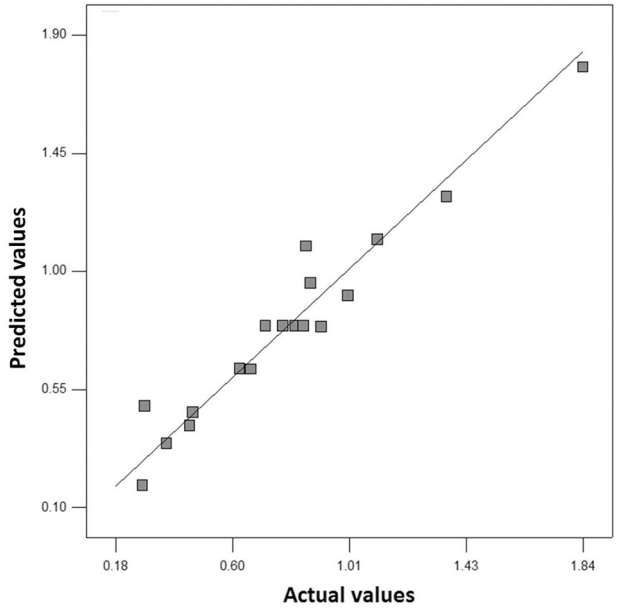

Fig. 4. Predicted vs. measured values of the corrosion rate in the presence of the inhibitor. The straight line is a guide to the eyes.

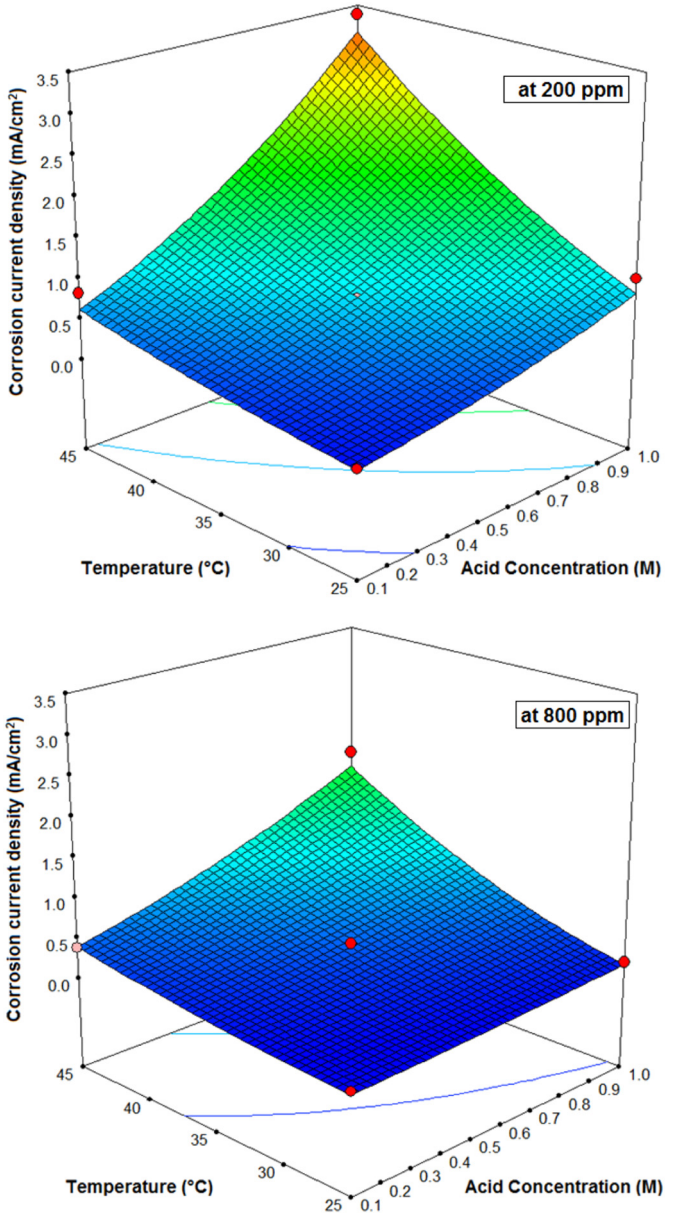

Fig. 5. Response surface for i_{corr} in the inhibited solutions based on the model presented in Table 4 at two inhibitor concentrations.

3.2. Uninhibited solution

Similar to the inhibited solutions, the corrosion potential of the St37 steel was measured in the blank solutions, the results of which are shown in Fig. 7. As can be seen from this figure, the corrosion potential in the absence of the inhibitor changes as a function of temperature and acid concentration. By increasing the temperature from 25 °C to 45 °C and acid concentration from 0.1 M to 1 M, the corrosion potential changes from −58 mV to −460 mV. Fig. 8 shows the results obtained

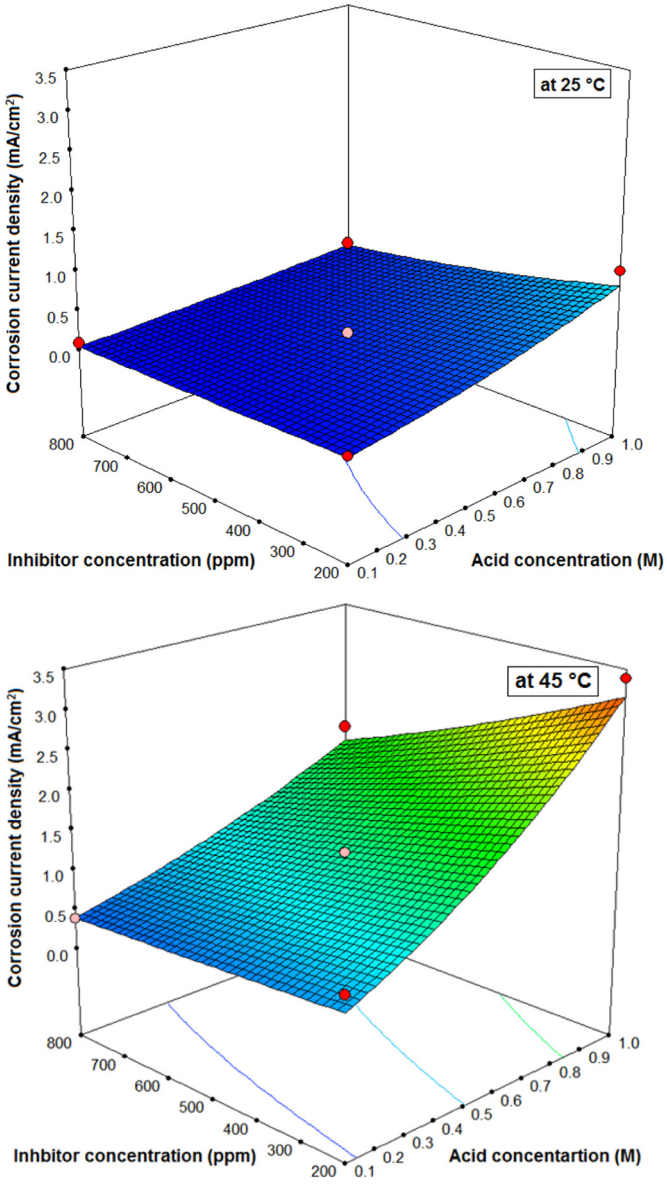

Fig. 6. Response surface for i_{corr} in the inhibited solutions based on the model presented in Table 4 at 25 °C and 45 °C.

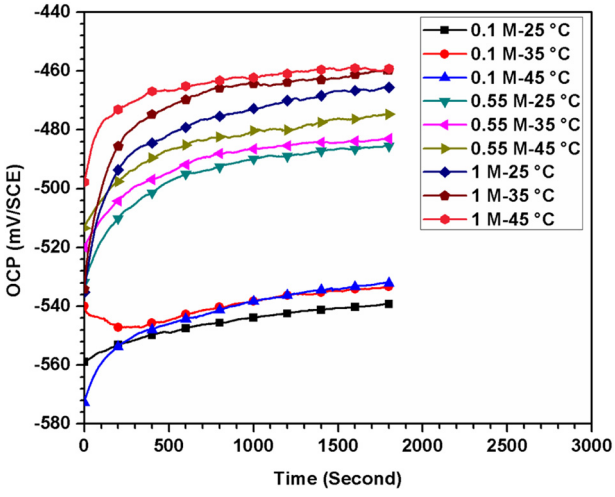

Fig. 7. Corrosion potential variations of the steel in different uninhibited solutions as a function of time.

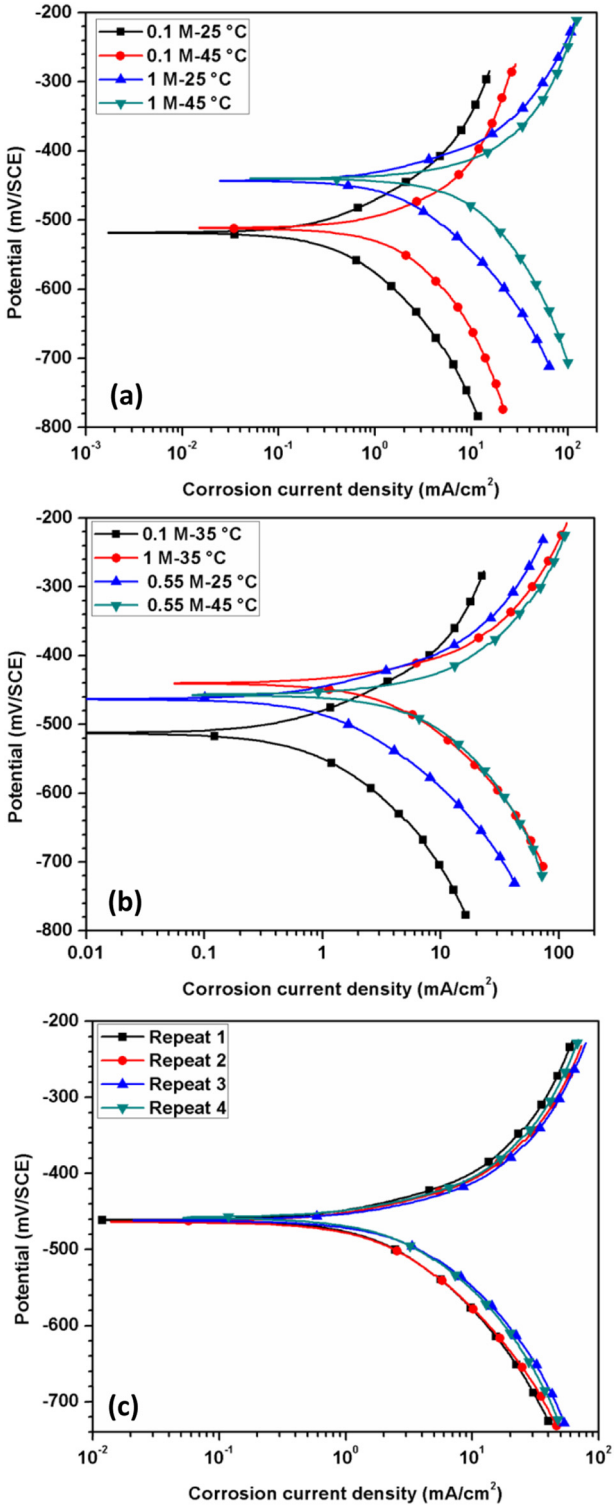

Fig. 8. Polarization curves of the mild steel in the blank solutions at the designed (a) factorial points, (b) star points, and (c) center points. The corresponding data can be found in Table 3.

from polarization tests in various conditions which were designed based on RSM method. Comparison between the corrosion current densities reported in Tables 2 and 3 reveals that at a similar condition, the corrosion rate is higher in the uninhibited solution than that in the inhibited solution. It is accepted generally that the corrosion rate decreases as the inhibitor molecules adsorb on the surface and block the

Table 5
Obtained model to calculate the corrosion rate in the uninhibited solutions.

Model Corrosion current density (mA/cm^2)	R-squared
$(i_{corr})^{0.5} = 2.19$ $-0.46 \times$ acid concentration $-0.12 \times$ temperature $0.06 \times$ acid concentration $\times$ temperature $+2\times10^3 \times (\text{temperature})^2$	0.96

active sites; the higher inhibitor concentration the higher surface blockage [28,29].

The influential parameters on which mathematical model is based are presented in Table 5. The model can predict the corrosion current density of the uninhibited sample as a function of acid concentration and temperature. The R-squared value of 0.96 indicates that this model is accurate enough to estimate the corrosion rate.

The predicted corrosion current densities are plotted versus the measured values in Fig. 9, showing a good correlation between the experiments and calculation. Fig. 10 depicts the corrosion rate for mild steel as a function of the acid concentration and the solution temperature. This figure demonstrates that a simultaneous increase in both acid concentration and temperature results in a significant rise in the corrosion current density. Nevertheless, at the low temperatures, the acid concentration does not affect the corrosion rate as much as it does at the elevated temperatures. This confirms the synergistic effects of the temperature and the acid concentration, as is considered in the obtained model [23].

3.3. The efficiency of the inhibitor

The inhibitive efficiency of an inhibitor highly depends on various environmental parameters including temperature, inhibitor concentration, and acid concentration. Thus, optimization of inhibited systems to function in various industrial conditions is of a great value. Fig. 11 shows the calculated inhibitive efficiency of the Clopidogrel as a function of the inhibitor concentration in various temperatures and pH values based on the established mathematical models. Since the two introduced mathematical models are able to calculate the corrosion rate of mild steel in

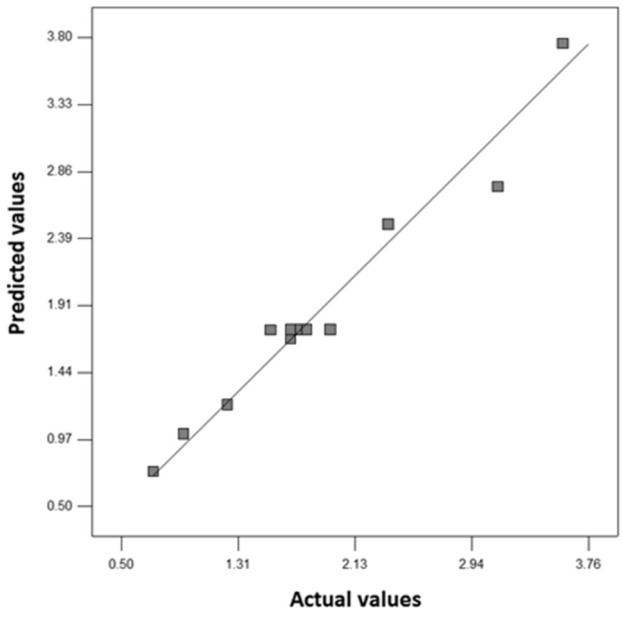

Fig. 9. Predicted vs. measured values of the corrosion rate in the absence of the inhibitor. The straight line is a guide to the eyes.

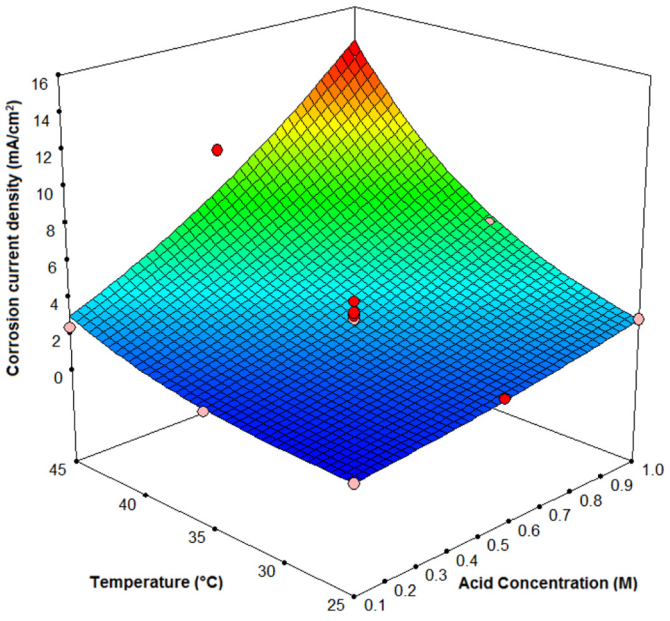

Fig. 10. Response surface for mild steel corrosion rate in uninhibited solutions based on the model presented in Table 5.

the presence and absence of the inhibitor in various conditions, the inhibitor efficiency can be calculated via the following equations [11]:

$$\theta = \frac{i_0 - i}{i_0} \quad (1)$$

$$\%\eta = \theta \times 100 \quad (2)$$

where η is the inhibitive efficiency, θ, is the surface coverage and the i_o and i are the corrosion rates in the absence and the presence of the inhibitor, respectively.

Comparison of the inhibitive efficiency of the 0.1 M solution at two different temperatures of 25 °C and 45 °C reveals that the inhibitor efficiency increases as the inhibitor concentration increases. However, as the temperature rises up to 45 °C, the inhibitive efficiency decreases steeply at the lower concentrations of the inhibitor. An acceptable efficiency is acquirable by increasing the inhibitor concentration, indicating the necessity of a critical minimum amount of inhibitor at higher temperatures. According to Fig. 11, in the 0.1 M solution, the inhibitive

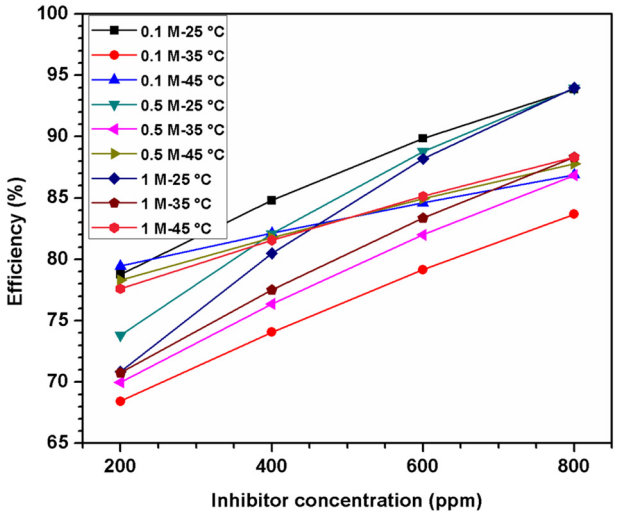

Fig. 11. Efficiency of Clopidogrel calculated in various conditions.

Table 6
Langmuir adsorption isotherm ΔG^{O}_{ads} calculated in various acid concentrations and temperatures.

Solution	0.1 M H_2SO_4			0.5 M H_2SO_4			1 M H_2SO_4		
Temperature (°C)	45	35	25	45	35	25	45	35	25
ΔG°_{ads} (kJ/ mol)	−34.95	−32.09	−31.05	−34.97	−31.05	−30.04	−34.92	−31.08	−30.04

efficiency of the compound decreases as the temperature rises up to 35 °C. At 45 °C, the inhibitive efficiency experiences some little changes by increasing the inhibitor concentration and it always remains between the efficiency of solutions at 25 °C and 35 °C. It is worth noting that the inhibitive efficiency is a non-linear function of the corrosion rate. Thus, the efficiency enhancement must not be interpreted as the reduction of the corrosion rate.

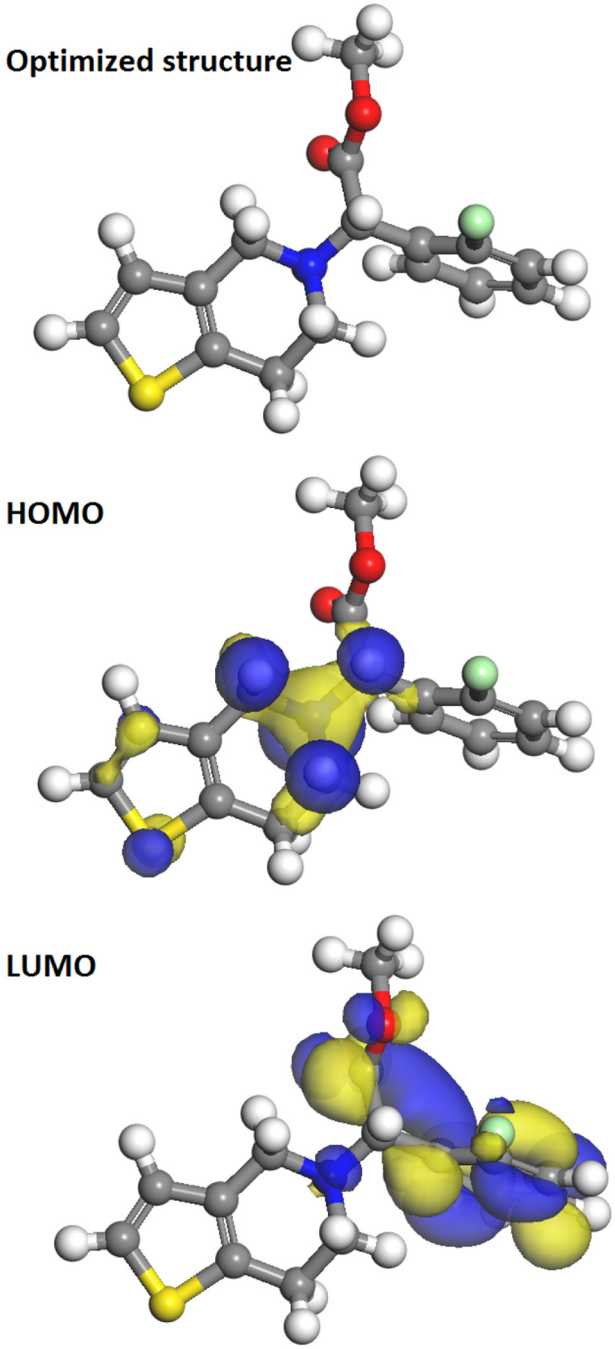

Fig. 12. Optimized structure, $E_{HOMO,}$ and E_{LOMO} of Clopidogrel.

In conclusion, Clopidogrel has a good ability to mitigate the steel corrosion even in server corrosive conditions and its efficiency reaches between 80% and 95% at 800 ppm in various conditions. In order to understand the inhibitive effect of Clopidogrel from a molecular point of view, we assessed the adsorption of Clopidogrel on steel surface by thermodynamic adsorption calculation and a combined MC simulation and spectroscopic studies.

3.4. Langmuir adsorption isotherm

Langmuir adsorption isotherm, which provides important information about the interactions between an inhibitor and a metal surface, is generally applied to the systems with inhibitors, because adsorption of inhibitor compounds mostly obeys this isotherm [30]. According to Langmuir isotherm, there is a relationship between the surface coverage, θ, and inhibitor concentration in mol/L, C, as is showed in Eq. (3) [11]:

$$\frac{C}{\theta} = \frac{1}{K} + C \tag{3}$$

The value of the equilibrium constant, K_{ads}, which can be calculated from the reciprocal of the intercept of C/θ-axis is used to estimate the

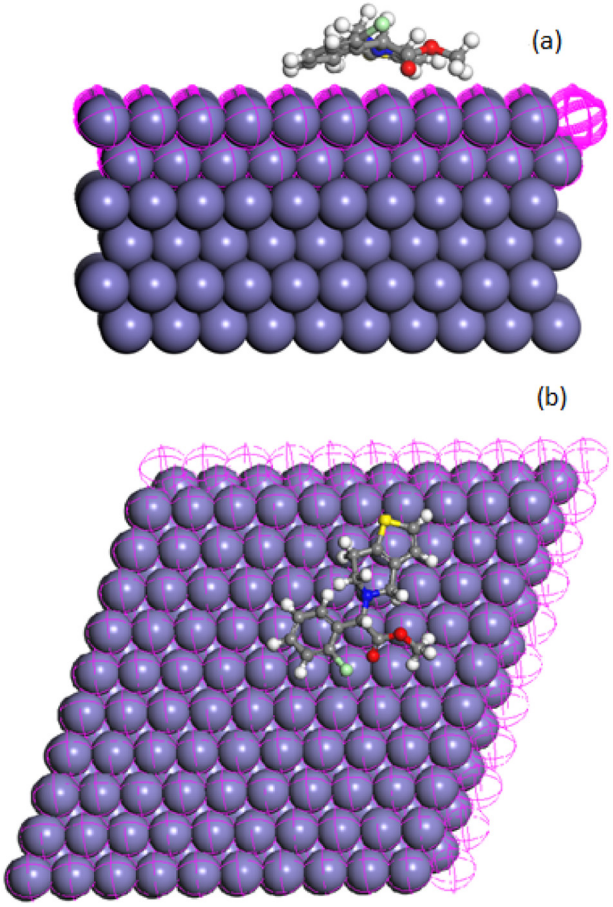

Fig. 13. Adsorption configuration of Clopidogrel in vacuum on Fe (100) plane (a) top view, and (b) side view.

standard free energy of inhibitor adsorption, ΔG^0_{ads}, on the metal surface. The following equation is reported for the calculation of ΔG^0_{ads} at different temperatures.

$$\Delta G_{ads} = -RT \ \ln(55.5K) \quad (4)$$

where R is the gas constant and T is the absolute temperature. The factor 55.5 is the molar concentration of water in 1 L solution and ΔG_{ads} is the free adsorption energy.

The calculated free adsorption energies of Clopidogrel in different temperatures and acid concentrations are listed in Table 6. The adsorption energy values reported for all the conditions remain between −30 and − 35 kJ/mol, revealing that Clopidogrel molecules adsorb both chemically and physically onto the steel surface [3,15,31]. Increasing the temperature results in an increase in the adsorption energy, which shows a stronger tendency of Clopidogrel to be chemically adsorbed on the steel surface at higher temperatures [32]. Although the inhibitor efficiency of Clopidogrel varies in different conditions (Fig. 11), its adsorption type on the metal surface remains as mixed-type. This is evident from Table 6 where the free adsorption energy is always between −30 and −35 kJ/mol.

3.5. Quantum chemical calculations

Fig. 16 shows the optimized structure, the highest occupied molecular orbital (HOMO) and the lowest unoccupied molecular orbital (LUMO) of Clopidogrel. The optimized structure of Clopidogrel is complicated, comprising orthogonal aromatic modes twisted around the bridging C atom. The HOMO electron density is populated in the center of the molecule and in the vicinity of N atom while the LUMO is observed on the right side of the molecule according to Fig. 12. It is predicted that for the electron donation driven adsorption, Clopidogrel may adsorb through the center of the molecule, whereas, if electron acceptation dominates the adsorption mechanism, Clopidogrel should adsorb through favorite LUMO sites [16,33].

To get a better understanding of the adsorption mechanism, MC simulations are carried out. Fig. 13 shows the adsorption configuration of a single Clopidogrel molecule through vacuum on a Fe (100) plane. As can be seen, the molecule adsorbs on the surface in a configuration that grants the maximum coverage. This is an intrinsic way that the system uses to minimize the total energy and therefore the adsorbate becomes thermodynamically more stable.

Since in real systems the inhibitor and water molecules compete for surface adsorption, we added 50 water molecules to the simulation box, in order to study the adsorption of the inhibitors in an aqueous media more accurately. The result of this simulation is shown in Fig. 14. As can be seen, Clopidogrel is able to overcome the water molecules and adsorb on the metal surface by replacing the water molecules. This behavior is due to the great affinity of Clopidogrel to adsorb on the steel surface, as can be deduced from its free adsorption energies in Table 6. It is noticeable that the adsorption configuration of the inhibitor changes in the presence of the water molecules, compared to adsorption configuration in vacuum. The simulated adsorption configuration of the Clopidogrel on steel surface is further evaluated using SFG.

3.6. Spectroscopic evaluations

As was mentioned earlier, to experimentally verify the adsorption configuration of Clopidogrel on steel, we performed vibrational

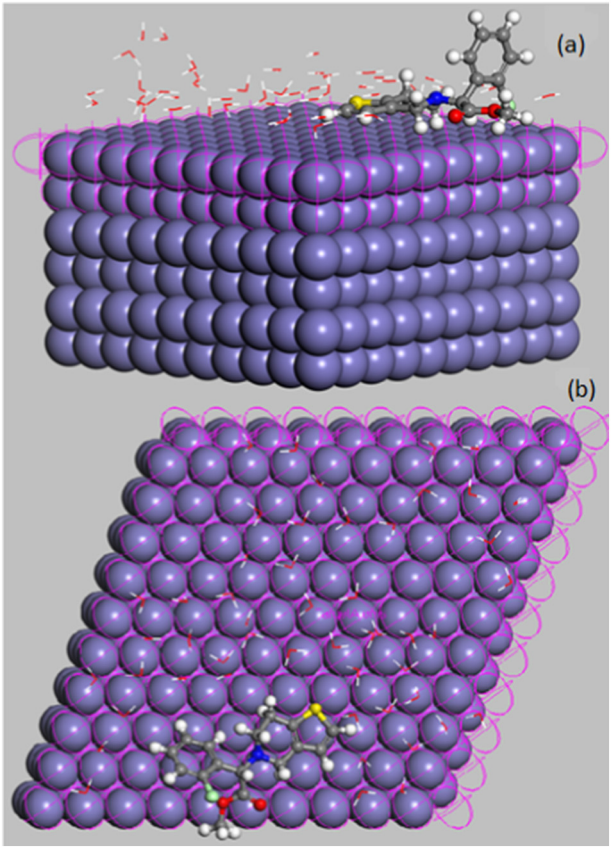

Fig. 14. Adsorption configuration of Clopidogrel in presence of water molecules on Fe (100) plane (a) top view, and (b) side view.

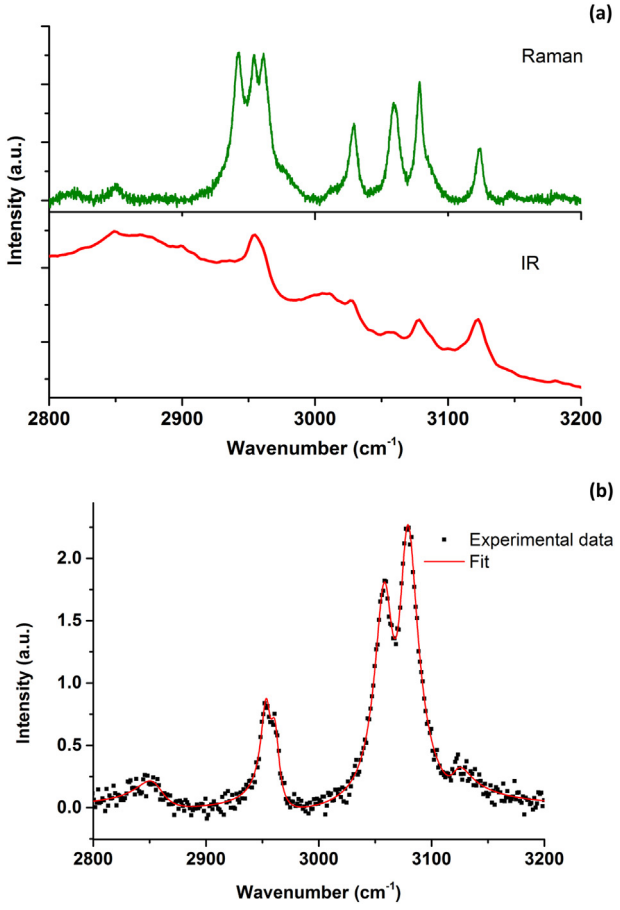

Fig. 15. (a) Raman (top) and IR spectra (bottom) of bulk Clopidogrel in the C—H stretching vibration frequency, and (b) SFG spectrum of Clopidogrel adsorbed on the surface of the steel. The black squares are the experimental point and the continuous red line represents the fit to the data. (For interpretation of the references to color in this figure legend, the reader is referred to the web version of this article.)

Table 7
IR and Raman peak assignments.

Mode	Raman peak position (cm^{-1})	IR peak position (cm^{-1})	SFG peak position (cm^{-1})
υ(CH) mode in the R1	3124	3121	3127
Symmetric stretch of $C_{11}H_{28}H_{29}$ group in R2	2850	2858	2850–2880
Asymmetric stretch of $C_{11}H_{28}H_{29}$ group in R2	2942	2912	–
υ(CH) mode in the R3	3058 and 3078	3057 and 3086	3059 and 3078
Vibration of $C_{13}H$ group connecting R2 and R3	2958	2953	2953
Symmetric and Asymmetric O-CH_3 group	2944, 3028 and 3048	–	3127

spectroscopic evaluations on a Clopidogrel-deposited steel surface. In linear vibrational spectroscopic methods, such as IR or Raman measurements, the signal will be overwhelmed by the bulk molecules, as the number of bulk molecules is way larger than those interacting with the substrate. Therefore, determining the configuration of adsorbed molecules would not be possible using linear spectroscopy. However, in SFG, owing to its selection rules, the SF signal is only generated where the symmetry is broken. In current study, only Clopidogrel molecules which are interacting with metal surface contribute to SF signal. Nevertheless, to be able to facilitate the SFG peak assignments, IR and Raman spectra were collected from the bulk Clopidogrel. Fig. 15(a) presents the Raman (top) and IR (bottom) spectra of bulk Clopidogrel in the C—H stretching frequency region. The main peak assignments are provided in Table 7. The SFG spectrum of the adsorbed Clopidogrel on the surface of steel is provided in Fig. 15(b) together with the fitted spectrum. The fit is performed using the fit equation described in [34]. It is worth noting that the only vibrational modes which are both IR and Raman active contribute to the SFG spectra. Furthermore, intensity of SFG signal depends on the specific orientation of vibrational modes with respect to the surface normal. As is observed in Fig. 15(b), vibrational modes arising from R3 (refer to Fig. 1) generate the most intense signal in the SFG spectrum. The observed SFG spectrum not only confirms that the Clopidogrel molecules are ordered at the metal interface, it also supports the results from MD simulation, where the R3 mode protrudes away from the metal surface. The absence of the vibrational modes from R1 and R2 confirms that these rings orient parallel to the sample surface. The assignment of the observed modes in the SFG spectrum is also provided in Table 7. Evaluation of the changes in the Clopidogrel configuration upon sample exposure to acidic medium can be followed using SFG both in-situ and ex-situ. However, this was not the scope of the current research and will be presented in our future publications.

3.7. Corrosion-attack-morphology study

Fig. 16 depicts the morphology of the mild steel surface after 90 min of immersion in various conditions. The mild steel surface without any inhibitor, Fig. 16(a), shows severe corrosion attacks after exposure to the acidic medium. In the presence of 800 ppm of inhibitor (Fig. 16(c)), the corrosion rate decreases considerably and the surface is etched slightly. Fig. 16(b) shows the mild steel after exposure to 1 M of sulfuric acid solution containing 200 ppm of inhibitor. As is obvious, the mild steel surface is corroded moderately as compared to Fig. 16(c). These figures demonstrate the effects of the inhibitor's presence and its concentration on the corrosion behavior of mild steel in acidic media.

4. Conclusions

In this study, RSM was employed to assess the environmental factors effect on the inhibitive performance of a cardiovascular drug (Clopidogrel), as a potential green inhibitor, for the steel corrosion in the acid sulfuric solution. Quantum chemical calculations and MC simulations are performed to get atomistic insight into the adsorption configuration of Clopidogrel on the steel surface. The simulation results are verified using inherent surface sensitive tool, sum frequency generation spectroscopy (SFG). The main findings are listed as follows:

1. The experimental models obtained through a statistical approach, RSM, are able to estimate the corrosion current density as a function of environmental factors, in the presence and the absence of the inhibitor. The models can further be used for estimation of surface coverages and subsequently thermodynamic calculation in a condition at which no experiment is conducted.
2. Clopidogrel reveals efficiencies between 80% and 95% in various environmental conditions; the efficiency rises as the inhibitor concentration increases. A strong correlation is found between acid concentration and temperature effect.
3. Clopidogrel adsorbs onto the steel surface in a mixed physical and chemical manner; this is deduced according to its calculated adsorption energy, which changes from −30 kJ/mol to −35 kJ/mol in different conditions. The inhibitive efficiency of the inhibitor is a function of exposure condition, but the adsorption type on the metal surface remains unchanged.

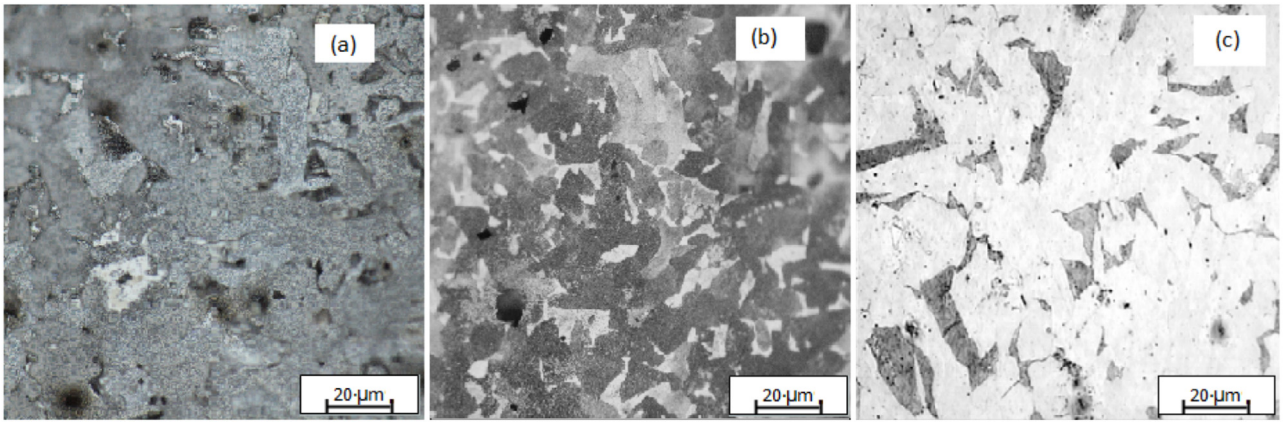

Fig. 16. Corrosion-attack-morphology of a mirror-like steel surface immersed for 90 min in (a) 0.1 M sulfuric acid, (b) 0.1 M sulfuric acid containing 800 ppm of inhibitor, and (c) 1 M sulfuric acid containing 200 ppm of inhibitor.

4. Quantum simulation demonstrated that Clopidogrel is able to adsorb on the metal surface by replacing the adsorbed water molecules. The configuration of adsorbed Clopidogrel molecules on the steel surface was evaluated experimentally using SFG. It was confirmed that Clopidogrel adsorbs on the surface with the R3 (Ring mode connected to Cl) standing away from the sample surface while the other ring modes (i.e. R1 and R1) arrange parallel to the surface.
5. The mild steel corrosion attack morphology studied in various conditions shows that the blank acidic solution can corrode the mirror-like steel surface severely after 90 min. The presence of inhibitor enhances the resistance of the surface against corrosion attack and this resistance was showed to be a function of inhibitor concentration.

Acknowledgements

We thank Prof. Wolfgang Peukert (FAU) for his valuable comments on our manuscript. SH also thanks Emerging Talents Initiative (ETI) 2018/2_Tech_06, FAU, Germany grant for supporting this research. Ferdowsi eUniversity of Mashhad is also acknowledged for providing the experimental facilities.

References

[1] G. Trabanelli, 1991 Whitney award lecture: inhibitors—an old remedy for a new challenge, Corrosion 47 (1991) 410–419.
[2] A.A. Olajire, Corrosion inhibition of offshore oil and gas production facilities using organic compound inhibitors - a review, J. Mol. Liq. 248 (2017) 775–808.
[3] F. Bentiss, M. Lagrenee, M. Traisnel, J.C. Hornez, The corrosion inhibition of mild steel in acidic media by a new triazole derivative, Corros. Sci. 41 (1999) 789–803.
[4] B.E. Amitha Rani, Bharathi Bai J. Basu, Green inhibitors for corrosion protection of metals and alloys: an overview, International Journal of Corrosion 2012 (2012).
[5] P.E. Laibinis, G.M. Whitesides, Self-assembled monolayers of n-alkanethiolates on copper are barrier films that protect the metal against oxidation by air, J. Am. Chem. Soc. 114 (1992) 9022–9028.
[6] S. Hosseinpour, M. Forslund, C.M. Johnson, J. Pan, C. Leygraf, Atmospheric corrosion of Cu, Zn, and Cu–Zn alloys protected by self-assembled monolayers of alkanethiols, Surf. Sci. 648 (2016) 170–176.
[7] Z.H. Gretić, E.K. Mioč, V. Čadež, S. Šegota, H. Otmačić Ćurković, S. Hosseinpour, The influence of thickness of stearic acid self-assembled film on its protective properties, J. Electrochem. Soc. 163 (2016) C937–C944.
[8] K. Cimatu, S. Baldelli, Spatially resolved surface analysis of an octadecanethiol self-assembled monolayer on mild steel using sum frequency generation imaging microscopy, J. Phys. Chem. C 111 (2007) 7137–7143.
[9] S. Hosseinpour, C.M. Johnson, C. Leygraf, Alkanethiols as inhibitors for the atmospheric corrosion of copper induced by formic acid: effect of chain length, J. Electrochem. Soc. 160 (2013) C270–C276.
[10] M. Göthelid, S. Hosseinpour, S. Ahmadi, C. Leygraf, C.M. Johnson, Hexane selenol dissociation on Cu: the protective role of oxide and water, Appl. Surf. Sci. 423 (2017) 716–720.
[11] S.K. Shukla, M.A. Quraishi, Cefalexin drug: a new and efficient corrosion inhibitor for mild steel in hydrochloric acid solution, Mater. Chem. Phys. 120 (2010) 142–147.
[12] Eno E. Ebenso, Arslan Taner, Kandemirli Fatma, Caner Necmettin, Love Ian, Quantum chemical studies of some rhodanine azosulpha drugs as corrosion inhibitors for mild steel in acidic medium, Int. J. Quantum Chem. 110 (2010) 1003–1018.
[13] Ashish Kumar Singh, Sudhish Kumar Shukla, M.A. Quraishi, Corrosion behaviour of mild steel in sulphuric acid solution in presence of ceftazidime, Int. J. Electrochem. Sci. 6 (2011) 5802–5814.
[14] K.F. Khaled, Monte Carlo simulations of corrosion inhibition of mild steel in 0.5 M sulphuric acid by some green corrosion inhibitors, J. Solid State Electrochem. 13 (2009) 1743–1756.
[15] A. Kosari, M. Momeni, R. Parvizi, M. Zakeri, M.H. Moayed, A. Davoodi, H. Eshghi, Theoretical and electrochemical assessment of inhibitive behavior of some thiophenol derivatives on mild steel in HCl, Corros. Sci. 53 (2011) 3058–3067.
[16] A. Ongun Yüce, B. Doğru Mert, G. Kardaş, B. Yazıcı, Electrochemical and quantum chemical studies of 2-amino-4-methyl-thiazole as corrosion inhibitor for mild steel in HCl solution, Corros. Sci. 83 (2014) 310–316.
[17] P. Singh, D.S. Chauhan, K. Srivastava, V. Srivastava, M.A. Quraishi, Expired atorvastatin drug as corrosion inhibitor for mild steel in hydrochloric acid solution, International Journal of Industrial Chemistry 8 (2017) 363–372.
[18] M. Abdallah, Rhodanine azosulpha drugs as corrosion inhibitors for corrosion of 304 stainless steel in hydrochloric acid solution, Corros. Sci. 44 (2002) 717–728.
[19] A.S. Fouda, W.M. Mahmoud, K.M.A. Elawayeb, Unused clopidogrel drug as eco-friendly corrosion inhibitor for carbon steel in aqueous media, Prot. Met. Phys. Chem. Surf. 53 (2017) 139–149.
[20] R.S. Dubey, K.U. Singh, Effect of clopidogrel on corrosion inhibition of mild steel in 1 M H_2SO_4, Asian J. Chem. 24 (4) (2012) 1759–1764.
[21] R.K. Pathak, Pratiksha Mishra, Drugs as corrosion inhibitors: a review, International Journal of Science and Research 5 (2016) 671–677.
[22] A. Srivastava, S. Mishra, P. Tandon, S. Patel, A.P. Ayala, A.K. Bansal, H.W. Siesler, Molecular structure and vibrational spectroscopic analysis of an antiplatelet drug; clopidogrel hydrogen sulphate (form 2) – a combined experimental and quantum chemical approach, J. Mol. Struct. 964 (2010) 88–96.
[23] A. Kosari, A. Davoodi, M.H. Moayed, R. Gheshlaghi, The response surface method as an experimental design technique to explore and model the performance of corrosion inhibitors, Corrosion 71 (2015) 819–827.
[24] S. Pongstabodee, S. Monyanon, A. Luengnaruemitchai, Applying a face-centered central composite design to optimize the preferential CO oxidation over a PtAu/CeO_2–ZnO catalyst, Int. J. Hydrog. Energy 37 (2012) 4749–4761.
[25] A.G. Lambert, P.B. Davies, D.J. Neivandt, Implementing the theory of sum frequency generation vibrational spectroscopy, Appl. Spectrosc. Rev. 40 (2005) 103–145.
[26] S. Hosseinpour, J. Hedberg, S. Baldelli, C. Leygraf, M. Johnson, Initial oxidation of alkanethiol-covered copper studied by vibrational sum frequency spectroscopy, J. Phys. Chem. C 115 (2011) 23871–23879.
[27] K. Engelhardt, W. Peukert, B. Braunschweig, Vibrational sum-frequency generation at protein modified air–water interfaces: effects of molecular structure and surface charging, Curr. Opin. Colloid Interface Sci. 19 (2014) 207–215.
[28] R. Solmaz, Investigation of the inhibition effect of 5-((E)-4-phenylbuta-1,3-dienylideneamino)-1,3,4-thiadiazole-2-thiol Schiff base on mild steel corrosion in hydrochloric acid, Corros. Sci. 52 (2010) 3321–3330.
[29] M.V. Azghandi, A. Davoodi, G.A. Farzi, A. Kosari, Corrosion inhibitive evaluation of an environmentally friendly water-base acrylic terpolymer on mild steel in hydrochloric acid media, Metall. Mater. Trans. A 44 (2013) 5493–5504.
[30] A. Fateh, M. Aliofkhazraei, A.R. Rezvanian, Review of corrosive environments for copper and its corrosion inhibitors, Arab. J. Chem. (2017) https://doi.org/10.1016/j.arabjc.2017.05.021 (In Press).
[31] M. Finšgar, D. Kek Merl, An electrochemical, long-term immersion, and XPS study of 2-mercaptobenzothiazole as a copper corrosion inhibitor in chloride solution, Corros. Sci. 83 (2014) 164–175.
[32] A. Kosari, M.H. Moayed, A. Davoodi, R. Parvizi, M. Momeni, H. Eshghi, H. Moradi, Electrochemical and quantum chemical assessment of two organic compounds from pyridine derivatives as corrosion inhibitors for mild steel in HCl solution under stagnant condition and hydrodynamic flow, Corros. Sci. 78 (2014) 138–150.
[33] G. Gece, The use of quantum chemical methods in corrosion inhibitor studies, Corros. Sci. 50 (2008) 2981–2992.
[34] S. Hosseinpour, M. Schwind, B. Kasemo, C. Leygraf, C.M. Johnson, Integration of quartz crystal microbalance with vibrational sum frequency spectroscopy–quantification of the initial oxidation of alkanethiol-covered copper, J. Phys. Chem. C 116 (2012) 24549–24557.